Journal of Petroleum Research and Studies

journal homepage: https://jprs.gov.iq/index.php/jprs/

Print ISSN 2220-5381, Online ISSN 2710-1096

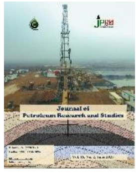

Machine Learning and Flow Zone Indicator for Permeability Estimation in Uncored Intervals of a Southern Iraqi Oil Field

Mohammed Rajaa*, Ayad A. Al-haleem

Department of Petroleum Engineering, College of Engineering, University of Baghdad, Baghdad, Iraq.

*Corresponding Author E-mail: mohammed.abd2408m@coeng.uobaghdad.edu.iq

Article Info

Received 23/01/2025
Revised 09/03/2025
Accepted 11/04/2026
Published 21/09/2026

DOI: http://doi.org/10.52716/jprs.v16i3.1075

Abstract

The precise estimation of permeability is a difficult task due to the nature of heterogeneous reservoirs. Attributable to the high costs of core sampling and the poor accuracy of the linear regression method, the Flow Zone Indicator (FZI) method is regarded as one of the most commonly used techniques in Iraqi fields in recent years to predict permeability. However, this method requires statistical or machine learning to predict FZI in uncored intervals. This study aims to identify the most suitable machine learning model for FZI prediction in uncored intervals using conventional well logs as input. Following this, the reservoir is divided into hydraulic flow units (HFUs) using unsupervised learning. Specifically, AutoGluon is used as an automated machine learning framework to find the best algorithm and optimal hyperparameters for FZI estimation. The k-means algorithm was employed to classify the reservoir into HFUs. This integrated approach was applied to a field case study in southern Iraq. The study utilized both core and log data from three wells. The results demonstrated that the neural network (NN) outperformed the other algorithms within the framework, achieving more than an R^2 of 90% and a root mean squared error (RMSE) of 1.69 on the test data, and more than an R^2 of 96% and an RMSE of 0.493 on the training data. By applying the derived correlations for each HFU, the permeability prediction achieved an R^2 of 85% and an RMSE of approximately 0.37. This demonstrates the effectiveness of the automated machine learning framework in improving FZI estimation and, consequently, permeability predictions.

Keywords: Flow Zone Indicator, hydraulic flow unit, Machine Learning, Permeability.

التعلم الآلي ومؤشر منطقة التدفق لتقدير النفاذية في فترات غير مستخرج اللباب من حقل نفطي جنوب العراق

الخلاصة:

إن التقدير الدقيق للنفاذية مهمة صعبة بسبب طبيعة الخزانات غير المتجانسة. ونظراً للتكاليف العالية لأخذ اللباب وضعف دقة طريقة المعادلة الخطية البسيطة، اعتبرت طريقة مؤشر منطقة التدفق (FZI) واحدة من أكثر التقنيات استخداماً في الحقول العراقية في السنوات الأخيرة للتنبؤ

بالنفاذية. ومع ذلك، تتطلب هذه الطريقة التقنيات الإحصائي أو التعلم الآلي للتنبؤ (FZI) في الاعماق غير مستخرجة اللباب. تهدف هذه الدراسة إلى تحديد نموذج التعلم الآلي الأكثر ملاءمة للتنبؤ بال(FZI) في الاعماق غير مستخرجة اللباب باستخدام سجلات الآبار التقليدية كمدخلات. بعد ذلك، يتم تقسيم الخزان إلى وحدات تدفق هيدروليكية (HFUs) باستخدام التعلم غير الخاضع للإشراف. على وجه التحديد، يتم استخدام AutoGluon كإطار عمل تعلم الآلي المؤتمت لإيجاد أفضل خوارزمية ومعلمات فائقة مثالية لتقدير (FZI). تم استخدام خوارزمية k-means لتصنيف الخزان إلى وحدات تدفق هيدروليكية. تم تطبيق هذا النهج المتكامل على دراسة حالة ميدانية في جنوب العراق. استخدمت الدراسة كل من البيانات الأساسية والسجلية من ثلاث آبار. وأظهرت النتائج أن الشبكة العصبية (NN) تفوقت على الخوارزميات الأخرى ضمن الإطار، حيث حققت أكثر من R^2 بنسبة 90٪ وخطأ جذر متوسط التربيع (RMSE) ب 1.69 على بيانات الاختبار، وأكثر من R^2 بنسبة 96٪ وRMSE ب 0.493 على بيانات التدريب. من خلال تطبيق الارتباطات المشتقة لكل HFU، حقق التنبؤ بالنفاذية R^2 بنسبة 85٪ وRMSE بنحو 0.37. وهذا يوضح فعالية إطار التعلم الآلي المؤتمت في تحسين تقدير FZI، وبالتالي التنبؤ بالنفاذية.

1. Introduction

Field development plans require decisions based on a reliable model that accurately represents the reservoir. Permeability is the most important property as it determines the reservoir's flow capacity. However, the inherent heterogeneity of permeability complicates and adds uncertainty to the reservoir characterization [1], [2].

Permeability is determined most accurately through direct calculation using core samples. However, the high cost and extensive time required for this approach make it impractical for all intervals. As a result, permeability in uncored intervals is typically estimated using well logs with statistical or theoretical models. One of the techniques used in permeability estimation is the hydraulic flow units (HFU) method. This method groups rocks that have similar flow characteristics and petrophysical properties into separate units [3]. Amaefule et al. developed this method, with each HFU defined by Flow Zone Indicator (FZI) [4]. The HFU method has been used for permeability prediction and rock-type classification in many studies of Iraqi fields [1], [5], [6], [7], [8], superiority over classical methods (e.g., linear regression) and machine learning (e.g., neural network (NN)) [9].

The HFU method is determined from core samples [10], [11]; therefore, it can be a poor representation of the reservoir because it depends on a statistical method to estimate FZI in uncored intervals. This limitation is highlighted by a comparative study of two reservoir simulation models [12]. One is NN-based for permeability estimation, and the other is HFU-based. The study found the NN-based model with an R^2 of 74% matched history production data better than the HFU-based model with an accurate R^2 of 92%. However, using machine learning for direct estimation of permeability can be unacceptably inaccurate in highly heterogeneous reservoirs. Alameedy et al. (2023) reported that the NN approach achieved an R^2 of approximately 62% in such cases [13].

Therefore, the objective of this study is to develop an approach that combines the generalization of machine learning models and the accuracy of the HFU method. Initially, FZI is calculated using porosity and permeability from core data. Subsequently, machine learning models are trained to find the value of FZI in uncored intervals using log data as input. Then, HFU is identified using unsupervised machine learning. Finally, distinct permeability prediction equations are derived for each identified HFU. The AutoGluon framework is employed to find the best model to predict FZI and use the K-clustering method to identify HFU. The following sections show the area of study, methodology and workflow, results that involve the most accurate method for FZI prediction, permeability predicted vs. core permeability, and conclusion.

1.1. Study area and Data

The Field X, discovered in 1977, is considered one of the five main fields in Dhi Qar Governorate. It is an untapped hydrocarbon resource with an area of 120 square kilometers. As shown in Figure (1), the field is 250 kilometers from southeast Baghdad, 26 kilometers from the north of Al-Rifai city, 16 kilometers from Qalaat Sukkar city, and 17 kilometers from the southwest of the Al-Dujail field. The field’s coordinates are 45.30° longitude and 31° latitudes [14], [15].

A number of studies have been conducted in the field, including an appraisal study or the construction of a three-dimensional geological reservoir model for several formations in the field, such as Nahr Umr, Zubair, Yamama, and Al-Mushrif [14], [15], [16], [17], [18], [19]. The Al-Zubair formation was selected for this study because it contains more than 1.5 billion barrels of oil and has a thickness of about 411 m [18], which necessitates a more precise permeability estimation for use in future development strategies.

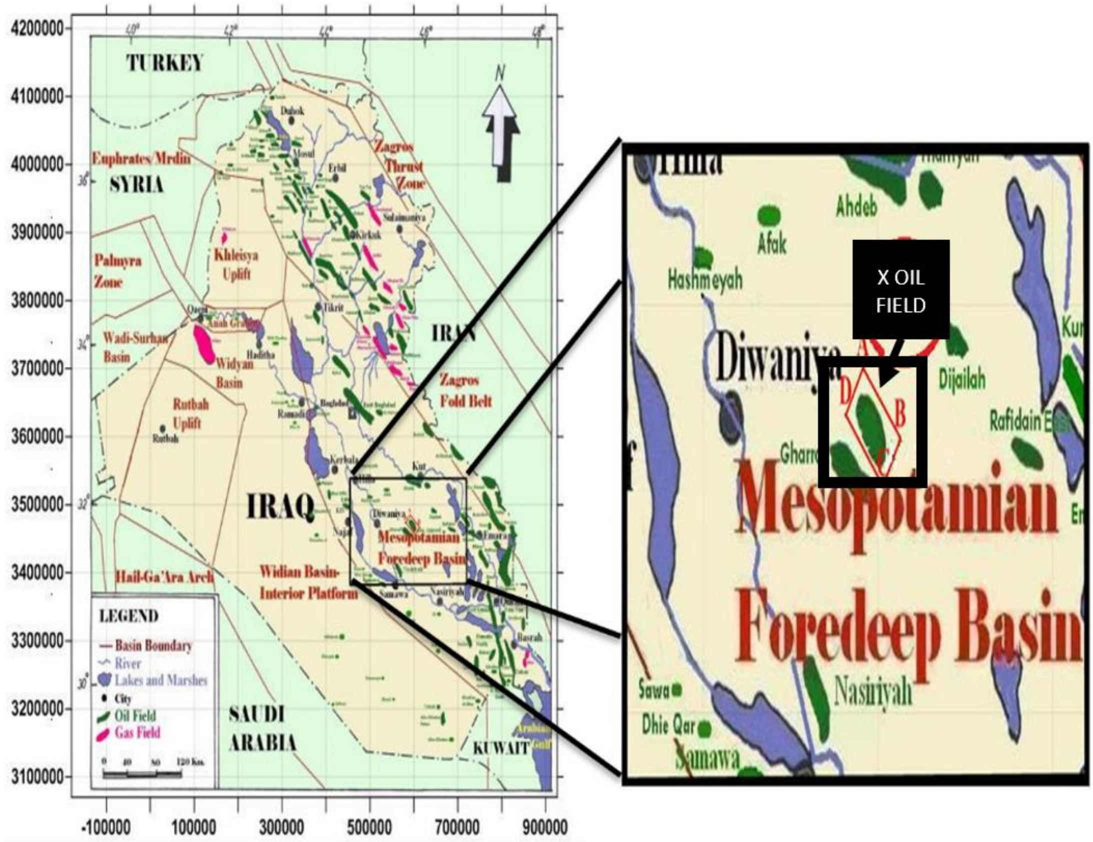

Fig. (1): Location of the study area x field [19]

The first well was drilled in 1980, which was followed by four wells at various locations. The data available in the field consist of conventional log data of all the 5 wells and core data of 3 wells at about 104 points, as shown in Table (1). Crossplot shows the relationship between the data, as shown in Figure (2), while the histogram shows the data distribution. The stratigraphic column in Figure (3) shows that sandstone, shale, and sandy shale are the dominant lithological types in the field.

Table (1): Data available and uses

variable	unit	use
Depth	m	unused
DT	US/F	
GR	API	
ILD	OHMM	
LLD	OHMM	Input
LLS	OHMM	(Supervised learning models)
NPHI	-	
RHOB	g/cm^3	
SFL	OHMM	
SP	OHMM	

Porosity	-	
FZI	-	Output (Supervised learning models)
HFU	-	Output (Unsupervised learning model)
Permeability	mD	Output (Correlations)

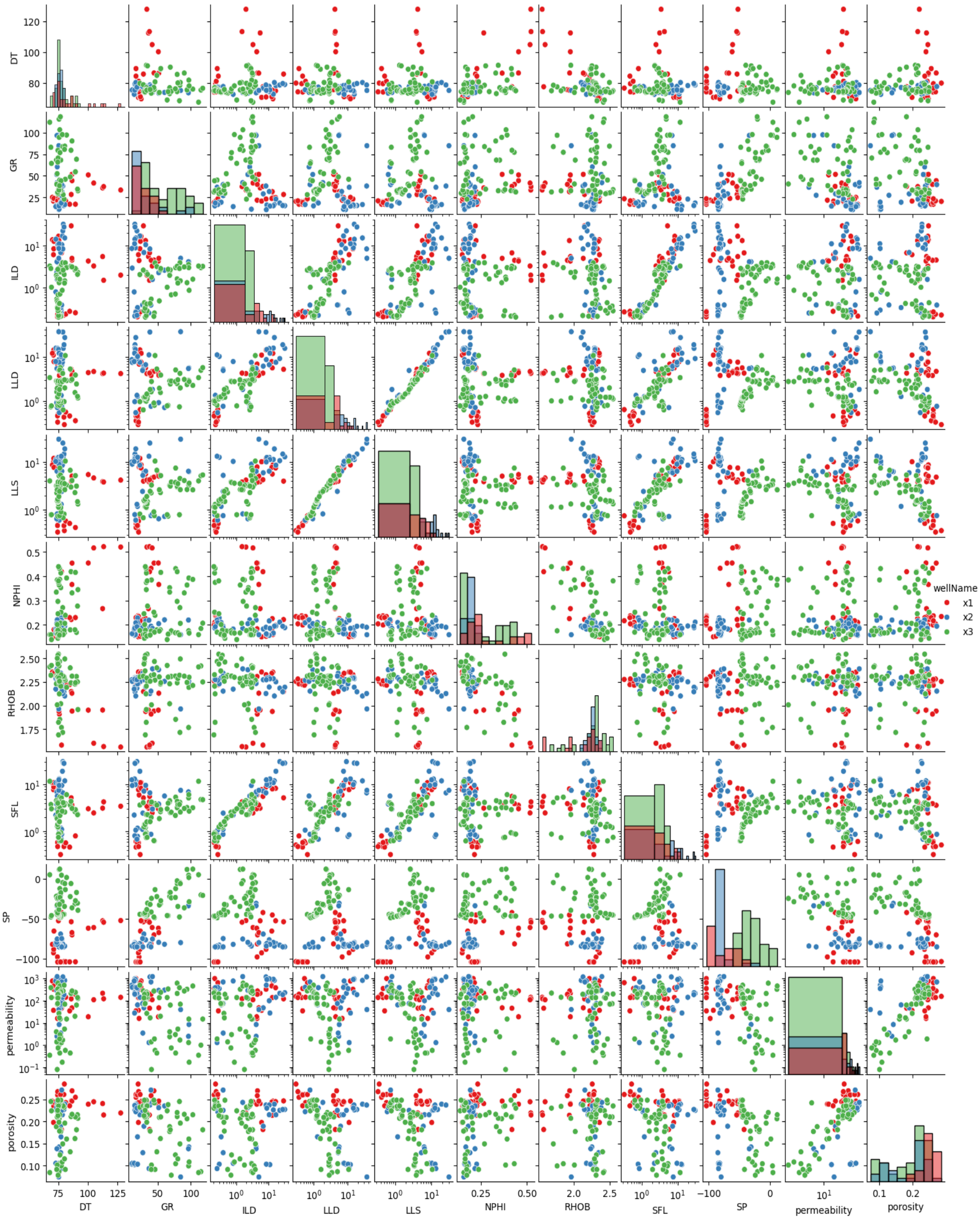

Fig. (2): Histograms and crossplots of core and log data: X-1, X-2, and X-3 wells

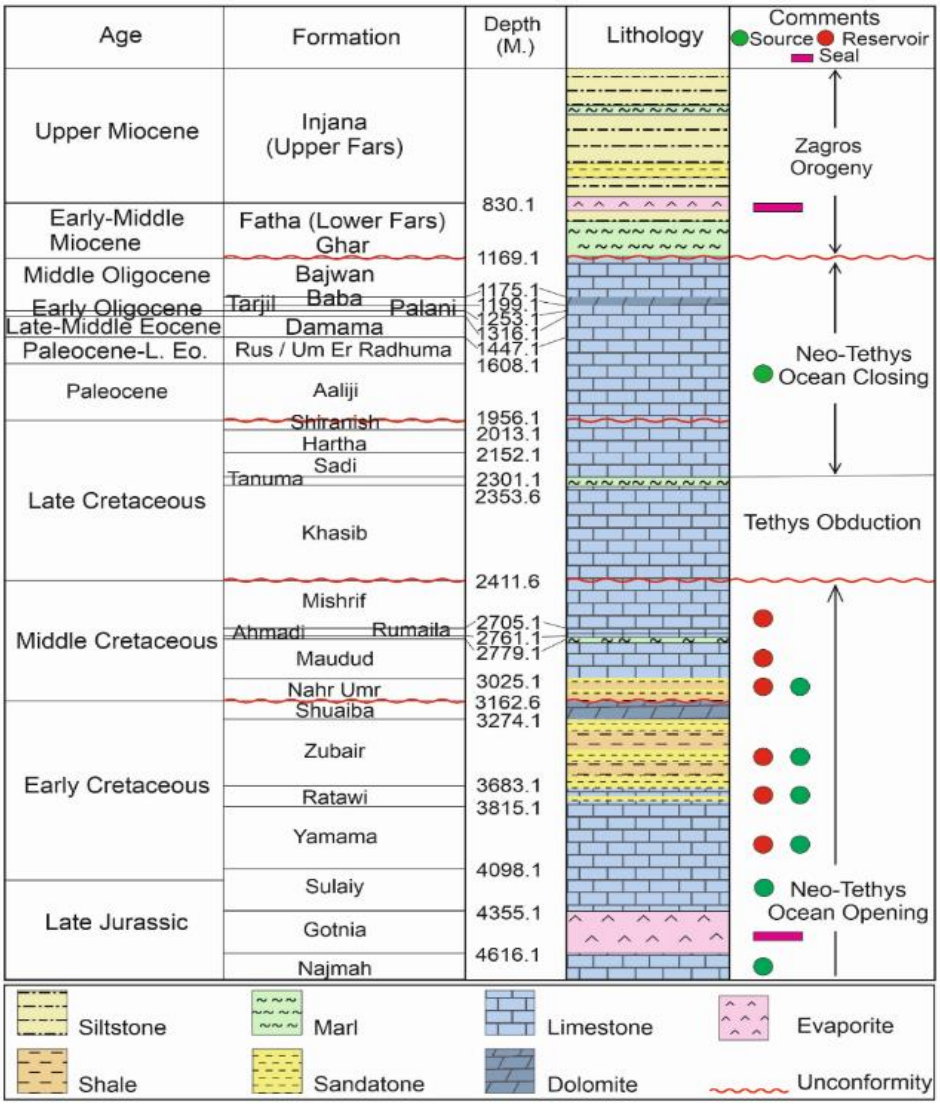

Fig. (3): X-1 well stratigraphic column [16]

2. Methodology

The methodology in this study is fundamentally illustrated in Figure (4), where it begins with the preparation of core data (including porosity and permeability) and the computation of the FZI value for each point in the cored interval. Subsequently, well logs are employed as inputs, and the computed FZI values as outputs to construct a machine learning model using the AutoGluon framework. The objective of employing the AutoGluon framework is to determine the optimal algorithm and hyperparameters for predicting FZI in the uncored interval. After calculating the FZI values in the uncored interval, the entire reservoir in each well is divided into HFUs using the K-clusters algorithm. Finally, an equation is derived to predict permeability from porosity for each HFU. In the following sections, the methods and tools utilized in the study will be explained.

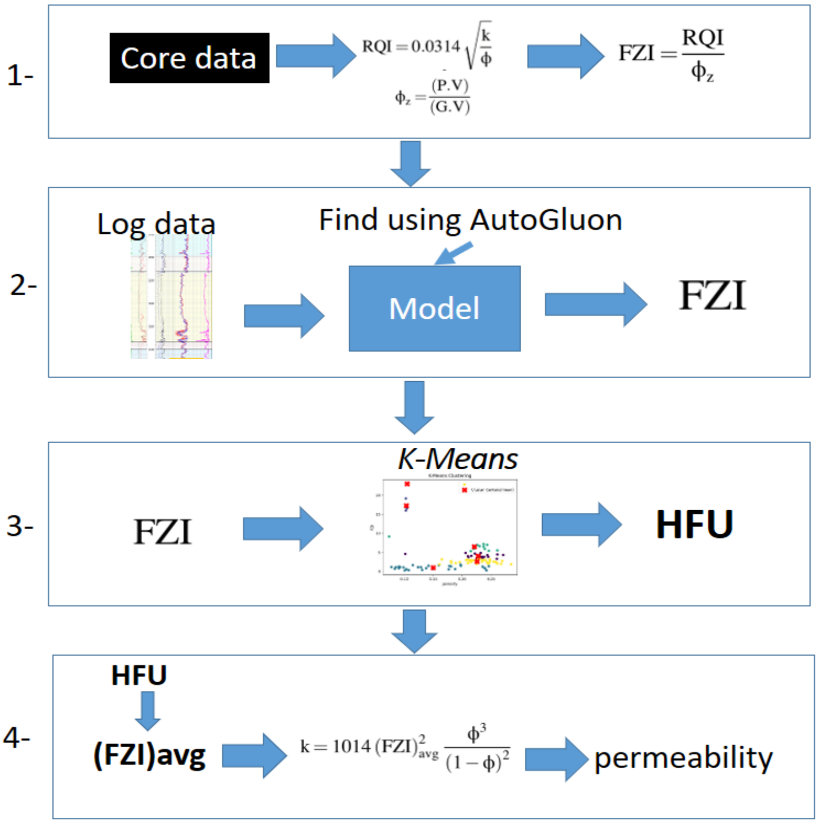

Fig. (4): Workflow of approach

2.1. HFU and FZI

the HFU method depends on three functions. Reservoir Quality Index (RQI), which was introduced by Amaefule et al. [20], is expressed by (1):

$$RQI = 0.314\sqrt{\frac{k}{\Phi}} \qquad (1)$$

Represent pore-throat size approximately [4]. Φ_Z expressed by (2):

$$\Phi_Z = \frac{\Phi}{1-\Phi} \qquad (2)$$

FZI [20], expressed by (3):

$$FZI = \frac{RQI}{\Phi_Z} \qquad (3)$$

Eq. 3 is linearized to plot Φ_Z and RQI on a log-log scale with many lines, each line with 45, having an average FZI value describing HFU, as shown in Figure (5).

By substituting 1 and 2 into eq. 3, the permeability can be calculated as (4):

$$k = 1014\,(FZI)^2{}_{avg}\,\frac{\Phi^3}{(1-\Phi)^2} \quad (4)$$

This equation will be used to calculate permeability in the final step of a workflow.

$$\log(RQI) = \log(\Phi_Z) + \log(FZI_{avg})$$

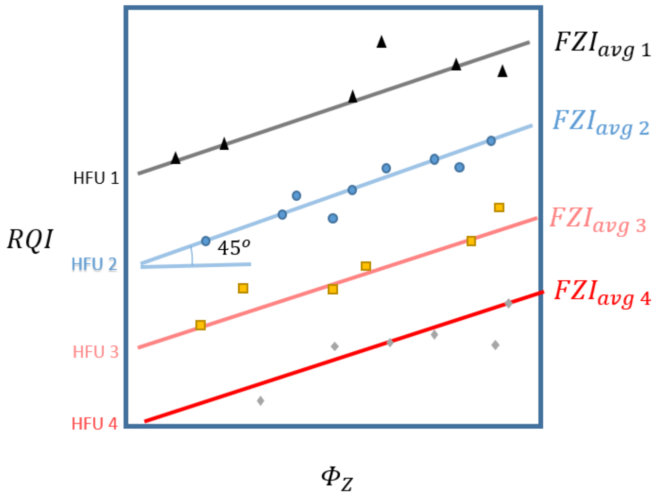

Fig. (5): Plot RQI and Φz on log-log scale with linearized eq. 3

However, using this method might not be feasible as shown in Figure (6) the points of X field data are overlapping. For this reason, the K-means algorithm was selected.

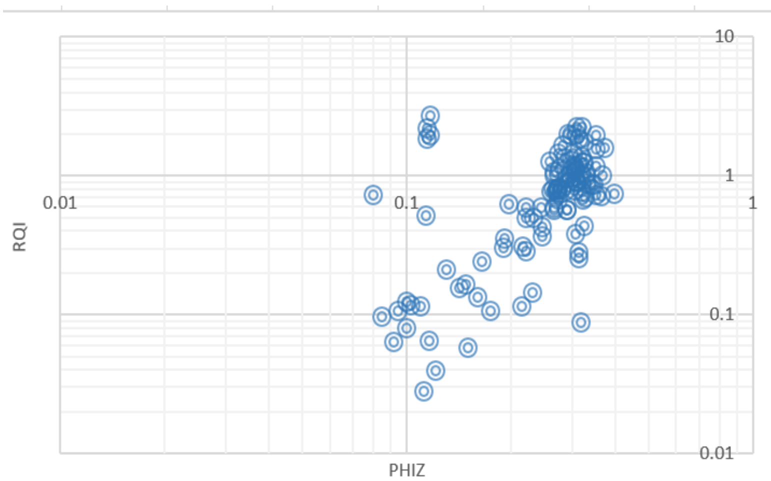

Fig. (6): RQI vs Φz plot for Zubair Formation

2.2. Machine learning

Machine learning algorithms can be divided into two types based on the learning method. In supervised learning, labels or outputs are provided to find the relationship between the input and output. AutoGluon was used to build several models. One of the automated machine learning frameworks for supervised learning algorithms was introduced by Amazon ML experts in 2020 [21]. This framework was chosen to predict the value of FZI to outperform many commercial automated frameworks. This framework creates a set of models with hyperparameter variations. It includes several modern machine-learning algorithms such as NN, CatBoost, Random Forest, Extra Trees, LightGBMXT, and XGBoost. The framework saves time and works with satisfactory results. The principle of the automated machine learning framework is shown in Figure (7), using a search algorithm to find the best algorithms, techniques, and hyperparameters. The objective function of this process is to find the best model to fit the data [22].

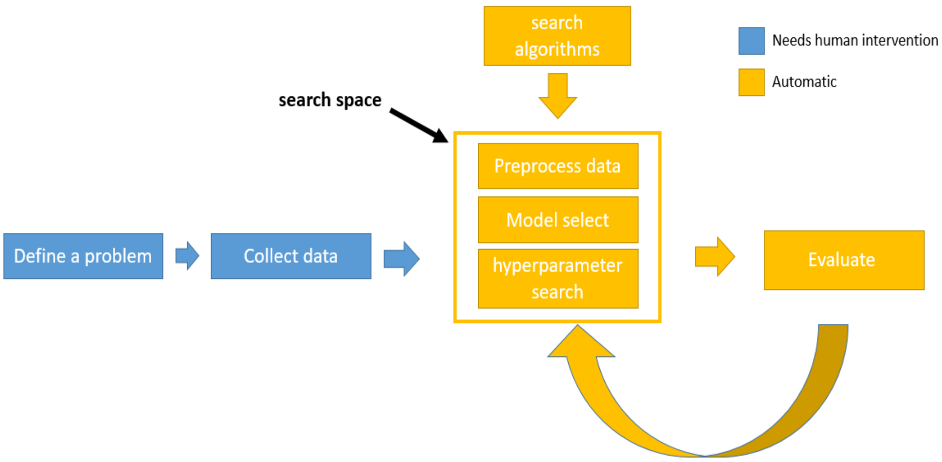

Fig. (7): Automatic method in training machine learning models

An unsupervised algorithm was used in this study. Learning, labels are not provided, and the objective function is to divide the data into similar groups. The K-means algorithm was used in this study. The principle of the algorithm is simple: after determining the required group divisions (K), the centroids of groups are randomly distributed. Then, each point is calculated distance with centroids, forming an initial cluster. The centroids are updated by calculating the average of the points until they stabilize and cannot be updated [23]. While the algorithm requires at least two inputs, log_{10}(FZI) and Probability of FZI were selected [2]. Also, the algorithm also requires predefining the number of clusters (*K*), a necessary parameter influencing the final clustering outcome. To determine the best number of K, the elbow method was applied [3]. This method involves iteratively executing the clustering algorithm for a range of K values, for example, from 2 to 16. For each iteration, after the clustering is performed, permeability is calculated for each cluster using Equation (4). R-squared is then calculated to assess the goodness of fit between the calculated permeability and the measured permeability from core samples, for each K value. The number of K is plotted against each R-squared value, and the point where further increases in K yield diminishing improvements in the R-squared value is called the elbow point.

2.3. Software and model selection criteria

The programs and tools used in this work include Techlog for preparing logs and core data and show the final results for comparison and matching between the actual and the predicted. Also, the Python programming language was used, and multiple libraries were used within it, such as Matplotlib and Seaborn for plotting, scikit-learn [24] for data splitting and calling the K-means algorithm, the AutoGluon framework for creating models, and Pandas for dealing with data.

In AutoGluon, test data and training data are used as the basis for the model selection criterion. Based on R-squared, the model performance can be divided into three levels. Above 0.9 represents an acceptable and excellent model, between 0.9 and 0.8 is considered good, and below 0.8 is considered poor [9]. However, this evaluation is not sufficient. Overfitting may occur due to a small training dataset, or it is the case that the model is complex on data [25]. Overfitting is recognized when the R-squared of the training data is higher than that of the test data. On the other hand, if the model is weak or there is an issue with the data distribution, both the R-squared of the training and test data will be poor. In addition, Equation 6 is also commonly used in many fields for evaluation representing the root mean squared error (RMSE), where the model with the lowest error value is selected [13]:

$$RMSE = \sqrt{\frac{\sum(yi - yp)^2}{n}} \qquad (5)$$

yi, is real permeability, yp is estimated permeability.

3. Results and Discussion

By involving the classic linear regression between porosity and permeability, as shown in Figure (8), the Zubair Formation is observed to be heterogeneous and has a weak relationship of about 49%. This led to the adoption of the HFU method for dividing the reservoir into units and creating a relationship for each one.

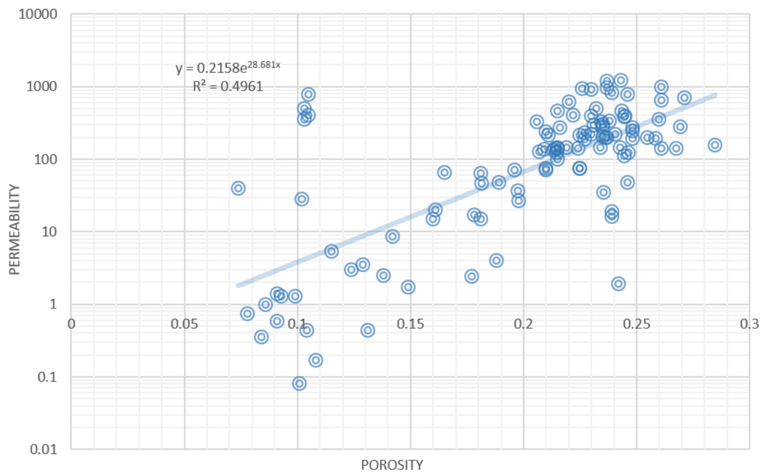

Fig. (8): Porosity and permeability relationship for Zubair Formation

In the following two sections, the results of what was mentioned in the workflow will be presented with discussion. For this reason, the K-means algorithm was selected.

3.1. FZI estimation

FZI was calculated for intervals with available core data using Eqs. 1, 2, and 3. To ensure model robustness, 20% of the data were randomly chosen and excluded from the training dataset. For each of the 4 machine learning algorithms employed, over 300 various hyperparameter combinations were tested. This resulted in the training and evaluation of over 1200 unique models. The best-performing model for each algorithm is presented in Table (2) and Figure (9).

Table (2): R^2 and RMSE for FZI estimated

	Train data		Test data	
Algorithm	R^2	RMSE	R^2	RMSE
NN	96.71%	0.493	90.09%	1.69
LightGBM	94.3%	0.644	84.09%	2.25
XGBoost	99.99%	0.001458	82.8%	2.34
CatBoost	95%	0.57	72.3%	2.96

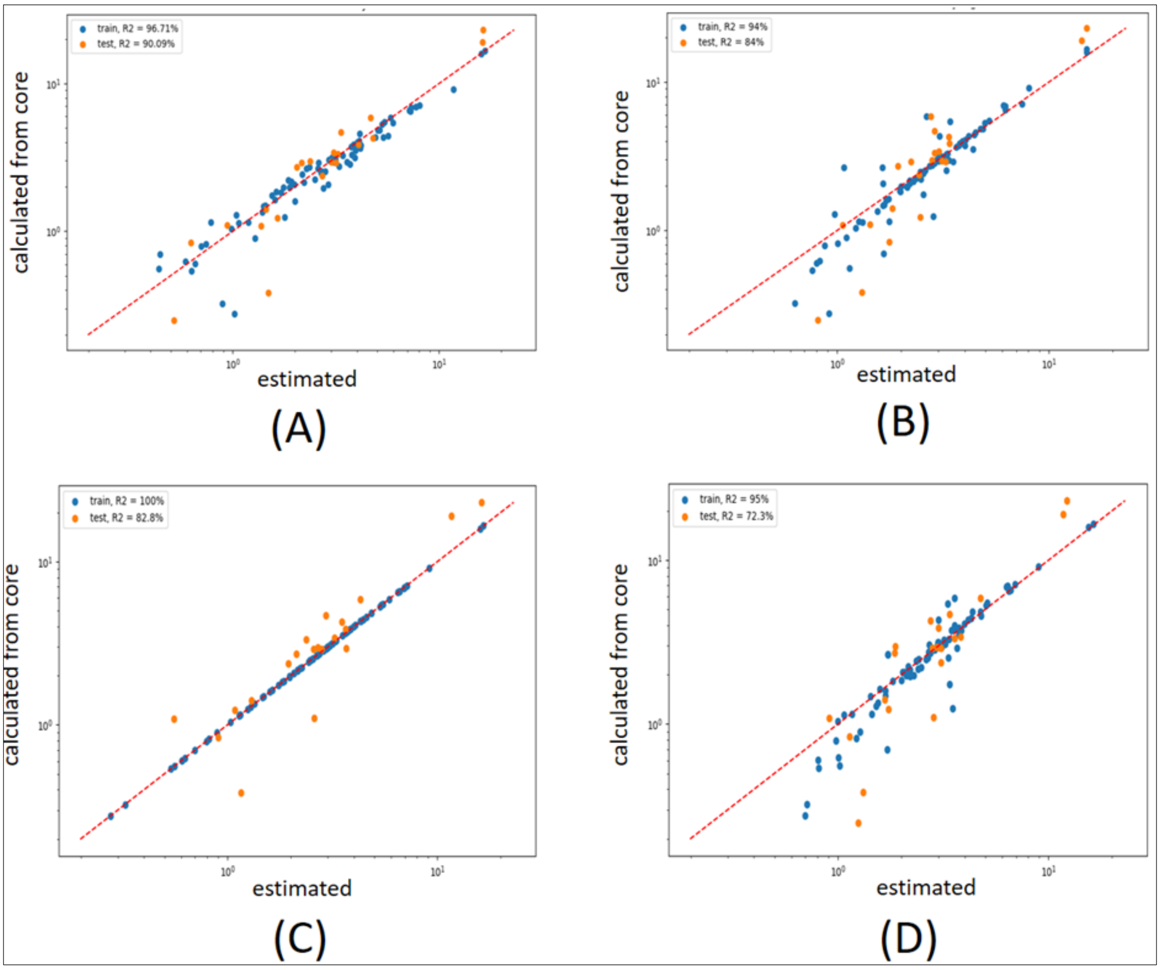

Fig. (9): Fit models on test and train data for: (A) NN (B) LightGBM (C) XGBoost (D) CatBoost

RMSE and R-squared were used to evaluate the performance of the models. All models exhibited superior performance on the training dataset. XGBoost achieved the best performance, as it had the lowest RMSE. In comparison, the models performance differed on the test data. LightGBM, XGBoost, and CatBoost overfit and decline performance. The NN model indicated the smallest difference in R-squared between the test and training data and achieved the best performance on the testing data. Thus, the NN model was selected for estimating FZI in the uncored intervals.

3.2. HFU and permeability calculation

Figure (10) shows the result of the elbow method, which was explained earlier, to determine the best clusters number of the FZI average.

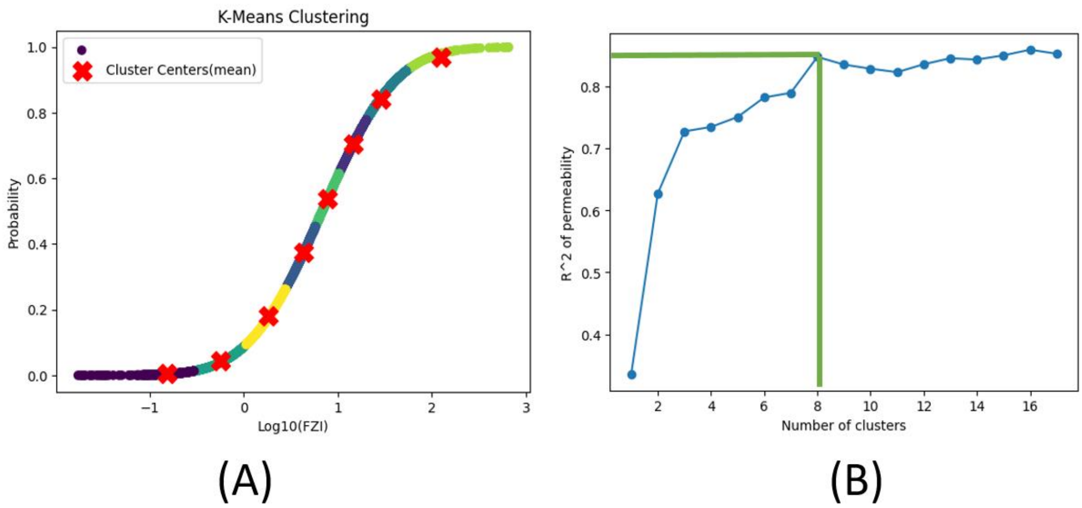

Fig. (10): Result of K-means algorithm, where: (A) represent log10(FZI) vs FZI with 8 clusters, (B) represent elbow method

The K-means result demonstrated the best K=8, with a permeability accuracy of about 84.7%. As Table 2 demonstrates, correlation can be generated for each HFU by applying the eq. 4. A crossplot between the actual permeability and the estimated permeability shown in Figure (11). The results of the R-squared was approximately 85%, and the RMSE was about 0.37. The match is displayed in Figure (12), where the results showed an acceptable agreement. The study was consistent with previous studies, where the NN model demonstrated superiority over the other models with an accuracy close to studies, such as direct permeability prediction with an accuracy of 87% [26], or prediction using FZI with machine learning with an accuracy of 86% [10]. This method outperformed previous studies that also employed machine learning in Iraq, such as using NN with Nuclear Magnetic Resonance (NMR) with an accuracy of 77% [27], using NN directly between log and core data with an accuracy of 74% [12], and also using NN with conventional log with an accuracy of 64% [13].

Table (2): Equation for each HFU

HFU	correlations
Cluster = 0	$k = 209.46 \dfrac{\Phi^3}{(1-\Phi)^2}$
Cluster = 1	$k = 10475.52 \dfrac{\Phi^3}{(1-\Phi)^2}$
Cluster = 2	$k = 3656.87 \dfrac{\Phi^3}{(1-\Phi)^2}$
Cluster = 3	$k = 18896.16 \dfrac{\Phi^3}{(1-\Phi)^2}$

Cluster = 4	$k = 639.51 \dfrac{\Phi^3}{(1-\Phi)^2}$
Cluster = 5	$k = 6075.59 \dfrac{\Phi^3}{(1-\Phi)^2}$
Cluster = 6	$k = 75542.82 \dfrac{\Phi^3}{(1-\Phi)^2}$
Cluster = 7	$k = 1742.92 \dfrac{\Phi^3}{(1-\Phi)^2}$

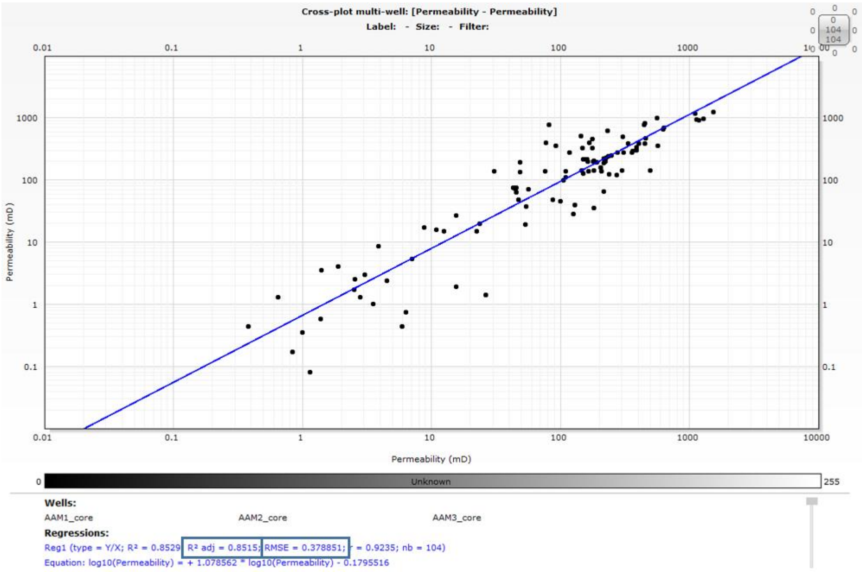

Fig. (11): Crossplot of permeability core vs predict

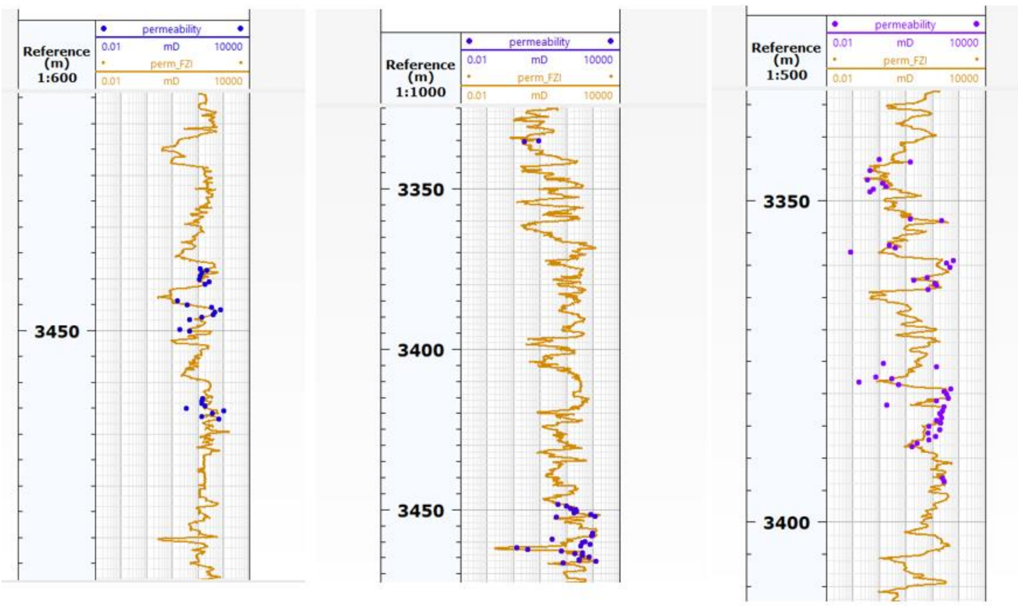

(A) (B) (C)

Fig. (12): Matching actual and predicted permeability, along depths as: (A) X-1 well, (B) X-2 well, (C) X-3 well

4. Conclusion

- The heterogeneous reservoirs make permeability more difficult to predict. To solve this problem, the FZI method was combined with machine learning techniques.
- Supervised learning algorithms were used to estimate FZI; the K-means algorithm as an unsupervised learning algorithm was involved in data clustering.
- By leveraging the AutoGluon framework, notable time and effort were conserved by automatically implicating hyperparameter optimization across numerous algorithms. The top 4 algorithms were shown, and the neural network had the best performance.
- This approach demonstrated satisfactory results, with a permeability prediction accuracy of approximately 85%. Using this approach can improve the accuracy of the reservoir model, leading to better reservoir management.

Author Contributions Statement: Mohammed Rajaa contributed to the Conception; Literature review; Experiments; Data Analysis; Writing – Original Draft. Ayad A. Al-haleem contributed to the Methodology; Data Interpretation; Writing – Review & Editing. All authors have read and approved the final version of the manuscript.

References

[1] A. M. Ali and A. A. Alhaleem, "Determination of Reservoir Hydraulic Flow Units and Permeability Estimation Using Flow Zone Indicator Method," *Iraqi Journal of Chemical and Petroleum Engineering*, vol. 24, no. 2, pp. 89–95, Jun. 2023, doi: https://doi.org/10.31699/IJCPE.2023.2.10.

[2] D. A. Alobaidi, "Permeability Prediction in One of Iraqi Carbonate Reservoir Using Hydraulic Flow Units and Neural Networks," *Iraqi Journal of Chemical and Petroleum Engineering*, vol. 17, no. 1, pp. 1–11, Mar. 2016, doi: https://doi.org/10.31699/IJCPE.2016.1.1.

[3] T. Astsauri, M. Habiburrahman, A. F. Ibrahim, and Y. Wang, "Utilizing machine learning for flow zone indicators prediction and hydraulic flow unit classification," *Scientific Reports*, vol. 14, no. 1, p. 4223, Feb. 2024, doi: https://doi.org/10.1038/s41598-024-54893-1.

[4] J. O. Amaefule, M. Altunbay, D. Tiab, D. G. Kersey, and D. K. Keelan, "Enhanced Reservoir Description: Using Core and Log Data to Identify Hydraulic (Flow) Units and Predict Permeability in Uncored Intervals/Wells," in *Proc. SPE Annual Technical Conference and Exhibition*, Houston, TX, USA, Oct. 3–6, 1993, Paper SPE-26436-MS, doi: https://doi.org/10.2118/26436-MS.

[5] Z. Mahdi and G. Farman, "Estimation of Petrophysical Properties for Zubair Reservoir in Abu-Amood Oil Field," *Iraqi Geological Journal*, vol. 56, no. 1B, pp. 32–39, Feb. 2023, doi: https://doi.org/10.46717/igj.56.1B.3ms-2023-2-11.

[6] H. Y. Ali and H. A. Chafet, "Predicting Permeability of the Mishrif Reservoir for Non-Cored Wells by Integrating Conventional Well Logs, Routine Core Analysis, and Drilling Data: A Case Study of Southeastern Iraq," *Iraqi Geological Journal*, vol. 57, no. 2C, pp. 84–101, Sep. 2024, doi:

https://doi.org/10.46717/igj.57.2C.7ms-2024-9-15.

[7] S. H. Al-Rubiaa and M. F. Al-Shahwan, "Rock typing and prediction permeability using machine learning techniques in Mishrif Formation, southern Iraq," *IOP Conference Series: Earth and Environmental Science*, vol. 1300, no. 1, Art. no. 012040, 2024, doi: https://doi.org/10.1088/1755-1315/1300/1/012040.

[8] A. T. Saleh and M. S. Aljawad, "Permeability Estimation for Upper Shale Member in Southern Iraqi Oil Field Using Machine learning and Hydraulic Flow Units Methods," *Iraqi Geological Journal*, vol. 56, no. 2B, pp. 90–101, Aug. 2023, doi: https://doi.org/10.46717/igj.56.2B.7ms-2023-8-16.

[9] O. Salman, O. F. Hasan, and S. Al-Jawad, "Permeability Prediction in One of Iraqi Carbonate Reservoir Using Statistical, Hydraulic Flow Units, and ANN Methods," *Iraqi Journal of Chemical and Petroleum Engineering*, vol. 23, no. 4, pp. 17–24, Dec. 2022, doi: https://doi.org/10.31699/IJCPE.2022.4.3.

[10] Z. Zhang, H. Zhang, J. Li, and Z. Cai, "Permeability and porosity prediction using logging data in a heterogeneous dolomite reservoir: An integrated approach," *Journal of Natural Gas Science and Engineering*, vol. 86, p. 103743, Feb. 2021, doi: https://doi.org/10.1016/j.jngse.2020.103743.

[11] E. Hajibolouri, A. A. Roozshenas, R. Miri, A. Soleymanzadeh, S. Kord, and A. Shafiei, "Permeability modelling in a highly heterogeneous tight carbonate reservoir using comparative evaluating learning-based and fitting-based approaches," *scientific reports*, vol. 14, no. 1, Art. no. 10209, May 2024, doi: https://doi.org/10.1038/s41598-024-60995-7.

[12] M. R. Abdul Hameed and S. M. Hamd-Allah, "Studying the Effect of Permeability Prediction on Reservoir History Matching by Using Artificial Intelligence and Flow Zone Indicator Methods," *Iraqi Geological Journal*, vol. 56, no. 1E, pp. 9–21, May 2023, doi: https://doi.org/10.46717/igj.56.1E.2ms-2023-5-12.

[13] U. S. Alameedy, A. T. Almomen, and N. Abd, "Evaluating Machine Learning Techniques for Carbonate Formation Permeability Prediction Using Well Log Data," *Iraqi Geological Journal*, vol. 56, no. 1D, pp. 175–187, Apr. 2023, doi: https://doi.org/10.46717/igj.56.1D.14ms-2023-4-23.

[14] A. Hussain, M. E. Nasser, and G. Hassan, "Evaluation of Mishrif Reservoir in Abu Amood Oil Field, Southern Iraq," *Iraqi Journal of Science*, vol. 62, no. 12, pp. 4758–4768, Dec. 2021, doi: https://doi.org/10.24996/ijs.2021.62.12.14.

[15] M. Q. Abed Talib and M. S. Al-Jawad, "Unveiling the Potential: A Pioneering Investigation into Nahr Umr Formation in Abu Amood Field," *Iraqi Geological Journal*, vol. 57, no. 1F, pp. 272–285, Jun. 2024, doi: https://doi.org/10.46717/igj.57.1F.20ms-2024-6-29.

[16] Z. S. Alshammary, A. J. Al-Khafaji, and F. M. Al-Najm, "Characterization of the Yamama Reservoir in the Abu-Amood Oil Field, Nasiriya, Southern Iraq," *Iraqi Geological Journal*, vol. 57, no. 1C, pp. 14–28, Mar. 2024, doi: https://doi.org/10.46717/igj.57.1C.2ms-2024-3-14.

[17] M. E. Nasser, S. N. Al-Jawed, and M. F. Hassan, "Geological Modeling for Yamama Formation in Abu Amood Oil Field," *Iraqi Journal of Science*, vol. 58, no. 2C, Jun. 2017, doi: https://doi.org/10.24996/ijs.2017.58.2C.9.

[18] Z. A. Mahdi and G. M. Farman, "3D Geological Model for Zubair Reservoir in Abu-Amood Oil Field," *Iraqi Geological Journal*, vol. 56, no. 1B, pp. 40–50, Feb. 2023, doi: https://doi.org/10.46717/igj.56.1B.4ms-2023-2-12.

[19] Z. A. Mahdi, "Evaluation of Petrophysical Properties and Construction of a 3D Geological Model for Zubair Formation in Abu-Amood Oil Field," *M.Sc. thesis, Dept. of Petroleum Engineering*, Univ. of Baghdad, Baghdad, Iraq, 2022.

[20] B. S. Nabawy, A. M. K. Basal, M. A. Sarhan, and M. G. Safa, "Reservoir zonation, rock typing

and compartmentalization of the Tortonian-Serravallian sequence, Temsah Gas Field, offshore Nile Delta, Egypt," *Marine and Petroleum Geology*, vol. 92, pp. 609–631, Apr. 2018, doi: https://doi.org/10.1016/j.marpetgeo.2018.03.030.

[21] N. Erickson, J. Mueller, A. Shirkov, H. Zhang, P. Larroy, M. Li, and A. Smola, "AutoGluon-Tabular: Robust and accurate AutoML for structured data," *arXiv preprint arXiv:2003.06505*, 2020, doi: https://doi.org/10.48550/arXiv.2003.06505.

[22] M. Baratchi, C. Wang, S. Limmer, J. N. van Rijn, H. H. Hoos, T. Bäck, and M. Olhofer, "Automated machine learning: Past, present and future," *Artificial Intelligence Review*, vol. 57, no. 5, Art. no. 122, 2024, doi: https://doi.org/10.1007/s10462-024-10726-1.

[23] J. Blömer, C. Lammersen, M. Schmidt, and C. Sohler, "Theoretical analysis of the k-means algorithm—A survey," in *Algorithm Engineering: Selected Results and Surveys*, L. Kliemann and P. Sanders, Eds., vol. 9220, *Lecture Notes in Computer Science*. Cham, Switzerland: Springer, 2016, pp. 81–116, doi: https://doi.org/10.1007/978-3-319-49487-6_3.

[24] F. Pedregosa, G. Varoquaux, A. Gramfort, V. Michel, B. Thirion, O. Grisel, M. Blondel, P. Prettenhofer, R. Weiss, V. Dubourg, J. Vanderplas, A. Passos, D. Cournapeau, M. Brucher, M. Perrot, and É. Duchesnay, "Scikit-learn: Machine learning in Python," *Journal of Machine Learning Research*, vol. 12, no. 85, pp. 2825–2830, 2011.

[25] X. Ying, "An Overview of Overfitting and its Solutions," *Journal of physics: Conference series*, vol. 1168, no. 2, Art. no. 022022, Feb. 2019, doi: https://doi.org/10.1088/1742-6596/1168/2/022022.

[26] R. Rezaee and J. Ekundayo, "Permeability Prediction Using Machine Learning Methods for the CO2 Injectivity of the Precipice Sandstone in Surat Basin, Australia," *Energies* (Basel), vol. 15, no. 6, Art. no. 2053, Mar. 2022, doi: https://doi.org/10.3390/en15062053.

[27] M. M. Hashim, G. M. Farman, and A. Askar, "Artificial Neural Network Application to Permeability Prediction from Nuclear Magnetic Resonance Log," *Iraqi Geological Journal*, vol. 57, no. 2D, pp. 88–99, Oct. 2024, doi: https://doi.org/10.46717/igj.57.2D.7ms-2024-10-17.